CrossMark

ORIGINAL PAPER

Indian summer monsoon rainfall variability during 2014 and 2015 and associated Indo-Pacific upper ocean temperature patterns

Rashmi Kakatkar[1,2] · C. Gnanaseelan[1] · J. S. Chowdary[1] · Anant Parekh[1] · J. S. Deepa[1,2]

Abstract In this study, factors responsible for the deficit Indian Summer Monsoon (ISM) rainfall in 2014 and 2015 and the ability of Indian Institute of Tropical Meteorology-Global Ocean Data Assimilation System (IITM-GODAS) in representing the oceanic features are examined. IITM-GODAS has been used to provide initial conditions for seasonal forecast in India during 2014 and 2015. The years 2014 and 2015 witnessed deficit ISM rainfall but were evolved from two entirely different preconditions over Pacific. This raises concern over the present understanding of the role of Pacific Ocean on ISM variability. Analysis reveals that the mechanisms associated with the rainfall deficit over the Indian Subcontinent are different in the two years. It is found that remote forcing in summer of 2015 due to El Niño is mostly responsible for the deficit monsoon rainfall through changes in Walker circulation and large-scale subsidence. In the case of the summer of 2014, both local circulation with anomalous anticyclone over central India and intrusion of mid-latitude dry winds from north have contributed for the deficit rainfall. In addition to the above, Tropical Indian Ocean (TIO) sea surface temperature (SST) and remote forcing from Pacific Ocean also modulated the ISM rainfall. It is observed that Pacific SST warming has extended westward in 2014, making it a basin scale warming unlike the strong El Niño year 2015. The eastern equatorial Indian Ocean is anomalously warmer than west in summer of 2014, and vice versa in 2015. These differences in SST in both tropical Pacific and TIO have considerable impact on ISM

rainfall in 2014 and 2015. The study reveals that initializing coupled forecast models with proper upper ocean temperature over the Indo-Pacific is therefore essential for improved model forecast. It is important to note that the IITM-GODAS which assimilates only array for real-time geostrophic oceanography (ARGO) temperature and salinity profiles could capture most of the observed surface and subsurface temperature variations from early spring to summer during the years 2014 and 2015 over the Indo-Pacific region. This study highlights the importance of maintaining observing systems such as ARGO for accurate monsoon forecast.

1 Introduction

Indian Summer Monsoon (ISM) is characterized by reversal of wind system arising due to land-sea thermal contrast (e.g. Ananthakrishnan, 1970; Webster and Chou, 1980; Trenberth et al. 2006). ISM variability at different timescales strongly impact the agricultural activities over the Indian subcontinent region (Webster et al. 1998; Yang et al. 2008; Kim et al. 2012; Jiang et al. 2013). The ocean plays an active and major role in the monsoon variability through coupled air-sea interactions (e.g. Shukla 1975; Webster, 2006, Kothawale et al. 2008; Bawiskar, 2009). El Niño displays teleconnection with ISM rainfall (Pant and Parthasarathy 1981; Keshavamurthy 1982; Kripalani and Kulkarni 1997; Kumar et al. 1999, 2006). Over the tropical oceans, El Niño and Southern Oscillation (ENSO) plays a major role in modulating the ISM variability both on seasonal and intra-seasonal time scales. Observational and modelling studies showed that during El Niño, ISM rainfall is below normal (e.g. Rasmusson and Carpenter 1983; Ropelewski and Halpert 1987). Recent studies highlighted the importance of Indian Ocean in the interannual variability of ISM (Saji et al. 1999; Ashok et al. 2001; Gadgil et al. 2004;

✉ C. Gnanaseelan
    seelan@tropmet.res.in

[1] Indian Institute of Tropical Meteorology, Pune 411008, India

[2] Department of Atmospheric and Space Sciences, Savitribai Phule Pune University, Pune, India

Krishnan et al. 2006; Gadgil et al. 2007; Chowdary et al. 2015). According to India Meteorological Department (IMD), Indian rainfall was deficit in 2014 (88%) and 2015 (86%) (Pai and Bhan 2015; Varikoden et al. 2015). During the last 115 years, 2014–2015 was the fourth case reported for two consecutive all-India-deficient monsoon years. 1904–1905, 1965–1966 and 1986–1987 are the previous cases of consecutive below normal ISM rainfall years (Kothawale and Kulkarni 2014). The weak El Niño conditions persisted in 2014 summer, whereas 2015 was among the strongest El Niño years. Thus, understanding the mechanisms responsible for two deficit consecutive monsoons in a contrasting remote forcing from Pacific is important.

Since ISM is a coupled system, better initial condition prepared with optimal use of observations is important for the coupled model-based forecast. Many modelling studies have highlighted the significance of better initial conditions mainly the upper ocean thermal structure in improving the skill of model forecasts (Ji and Leetmaa 1997; Balmaseda et al. 2009; Balmaseda and Anderson 2009). Ji et al. (1998) showed improved ENSO prediction skill with improvement in the ocean initial conditions through improved ocean analysis system. Balmaseda et al. (2007) showed the improvement in the seasonal forecast skill of sea surface temperature (SST) over most of the global oceans using Array for Real-Time Geostrophic Oceanography (ARGO) data assimilation. ARGO is one of the major developments in the ocean observing systems, and deployment over the global oceans started in 2002. ARGO is an international project which collects high-quality continuous observations of ocean temperature and salinity profiles in the upper 2000 m of the ocean (Gould et al. 2004). ARGO has a good global coverage with greater than 3000 floats over the globe and at around 3° resolution (e.g. Roemmich et al. 1998; Roemmich and Gilson 2009, 2011). There are many studies highlighting the importance of ocean initialization in better forecasts (e.g. Ravichandran et al. 2011, 2013). The National Centres for Environmental Prediction (NCEP) Global Ocean Data Assimilation System (GODAS) is implemented at Indian Institute of Tropical Meteorology (IITM) for improving ocean initial condition for Climate Forecast System version 2 (CFSv2) (Sreenivas et al., 2015). This GODAS version at IITM (IITM-GODAS) assimilates ARGO temperature and salinity (instead of synthetic salinity) profiles. Assimilation using IITM-GODAS for the period from 2005 to 2014 resulted in improved analysis of the ocean state (Sreenivas et al. 2015). In this paper, we have analysed the ocean–atmosphere coupled mechanisms responsible for the 2014 and 2015 deficit ISM rainfall. The ocean state during these 2 years in IITM-GODAS has been examined. The paper is organized as follows. Data and model used in the study are described in Sect. 2. Section 3 examines the factors responsible for deficit ISM rainfall in 2014 and 2015. Representation of upper ocean temperature in IITM-GODAS is discussed in Sect. 4. Summary is provided in Sect. 5.

2 Data and model used in the study

Rain fall data used in this study are high-resolution (0.25° × 0.25°) rainfall over the Indian land region from IMD (Pai et al. 2014) and National Oceanic and Atmospheric Administration (NOAA) Climate Prediction Center (CPC) Merged Analysis of Precipitation (CMAP) of 2.5° × 2.5° spatial resolution (Xie and Arkin 1997). NOAA Climate Data Record (CDR) 2.5° × 2.5° monthly Outgoing Longwave Radiation (OLR) version 2.2-1 (Lee and NOAA CDR Program 2011) is used as a proxy for convection. Low OLR implies high convection and vice versa. Wind and mean sea level pressure (SLP) are obtained from the European Centre for Medium Range Weather Forecasts (ECMWF) re-analysis (ERA-Interim) (Dee et al., 2011). ERA-Interim is a global atmospheric reanalysis and it is updated continuously in real time. NOAA Optimum Interpolation Sea Surface Temperature (OISST) v2 high-resolution dataset (Reynolds et al. 2007) is also used in this study. The 0.25° × 0.25° daily OISST is an analysis constructed by combining observations from different platforms such as satellites, ships and buoys on a regular global grid. Met Office Hadley Centre observations/reanalysis dataset Had-EN4.1.1 ocean temperature is also used (Good et al. 2013). Had-EN4.1.1 data is quality-controlled subsurface ocean temperature and salinity profiles. In this study, ocean subsurface temperature analyses (with Levitus et al. (2009) corrections) are also utilized.

The GODAS is the ocean data assimilation module for CFS. It has Modular Ocean Model (MOM4p0) as ocean model. It uses 3D-Var data assimilation scheme and 0.5° resolution in zonal and meridional direction. Between 10°S to 10°N, meridional resolution is 0.25°. There are 40 vertical levels approximately up to 4400 m depth with 10-m resolution in the upper 240 m. The National Centre for Medium Range Weather Forecasting (NCMRWF) surface forcing is used to force for the period of 2010 to 2015. NCMRWF forcing is of 0.25° spatial resolution and six hourly temporal resolutions. Further, ARGO profiles are assimilated in IITM-GODAS (Khandekar et al. 2015; Sreenivas et al. 2015). The ARGO temperature and salinity profiles are obtained from Coriolis (http://www.coriolis.eu.org/).

CFSv2 is a coupled ocean atmosphere model (Saha et al., 2014). Its atmospheric component is Global Forecast System (GFS) with T126 horizontal resolution and 64 hybrid vertical levels. MOM4p0 is the oceanic component of CFSv2 (Griffies et al. 2004). CFSv2 hindcast runs are carried out with May initial conditions. A seven-members ensemble is used for the analysis. The dates of the members are 1st of May and 5th to 10th of May. The atmospheric initial conditions are taken from NCEP Operational Analysis (Behringer and Xue, 2004; Behringer, 2007). CFSv2 runs are carried out with IITM-GODAS and NCEP-GODAS ocean initial conditions for 2014 and 2015. The experiments are carried out on the high performance computer "Aaditya" at IITM.

3 Oceanic and atmospheric conditions in summer of 2014 and 2015

Spatial distributions of rainfall anomalies during the summer monsoon of 2014 and 2015 highlight the areas suffered by deficit rainfall over the Indian subcontinent and other South Asian monsoon regions (Fig. 1). Negative rainfall anomalies over the Indian land region are apparent in most of the summer (JJAS; June through September) season (Fig. 1a, b), suggesting that monsoon rainfall is deficit in the consecutive years 2014 and 2015. To understand the spatial distribution of rainfall over the Indo-Pacific region, CMAP rainfall anomalies are shown in Fig. 1c, d. Spatial distribution of rainfall over the Indian Ocean is different in these two years. In 2014, positive rainfall anomalies are seen over most of the Arabian Sea, southeast Indian Ocean, some parts of Bay of Bengal (Fig. 1c), and the Western Ghats region (Fig. 1a, c). In contrast, 2015 witnessed negative rainfall anomalies over most parts of the Arabian Sea and southeast Indian Ocean (Fig. 1d) and over the Indian land region (Fig. 1b). OLR anomalies show positive values over the Indian region in both the years but with a contrasting dipole

structure in the southern Indian Ocean (Fig. 1c, d). Negative OLR anomalies are seen in the southeast Indian Ocean in 2014 and in the southwest Indian Ocean in 2015. Over most of the Pacific Ocean, negative OLR anomalies are evident in both years. The SST anomalies (Fig. 1e, f) also display some important differences in the 2 years. In 2014, western equatorial Indian Ocean shows weak negative anomalies and rest of the Indian Ocean and most of the equatorial Pacific display positive SST anomalies. On the other hand, in 2015, basin wide warming was apparent in the Tropical Indian Ocean (TIO) with strong warming in the west and central region. Eastern equatorial Pacific Ocean is warm while western equatorial Pacific is cold, which represents typical El Niño-like conditions. Further, northwest Pacific is warm in 2014 while northeast Pacific is warm in 2015. Overall, El Niño conditions are strong over the Pacific in 2015 as compared to 2014. These El Niño conditions are known to have strong impact on ISM rainfall as displayed in Fig. 1a, b. It is noted that the TIO SST response to El Niño is different during 2014 and 2015 partly due to the differences in the El Niño strength. To understand further the mechanisms, the atmospheric state is studied.
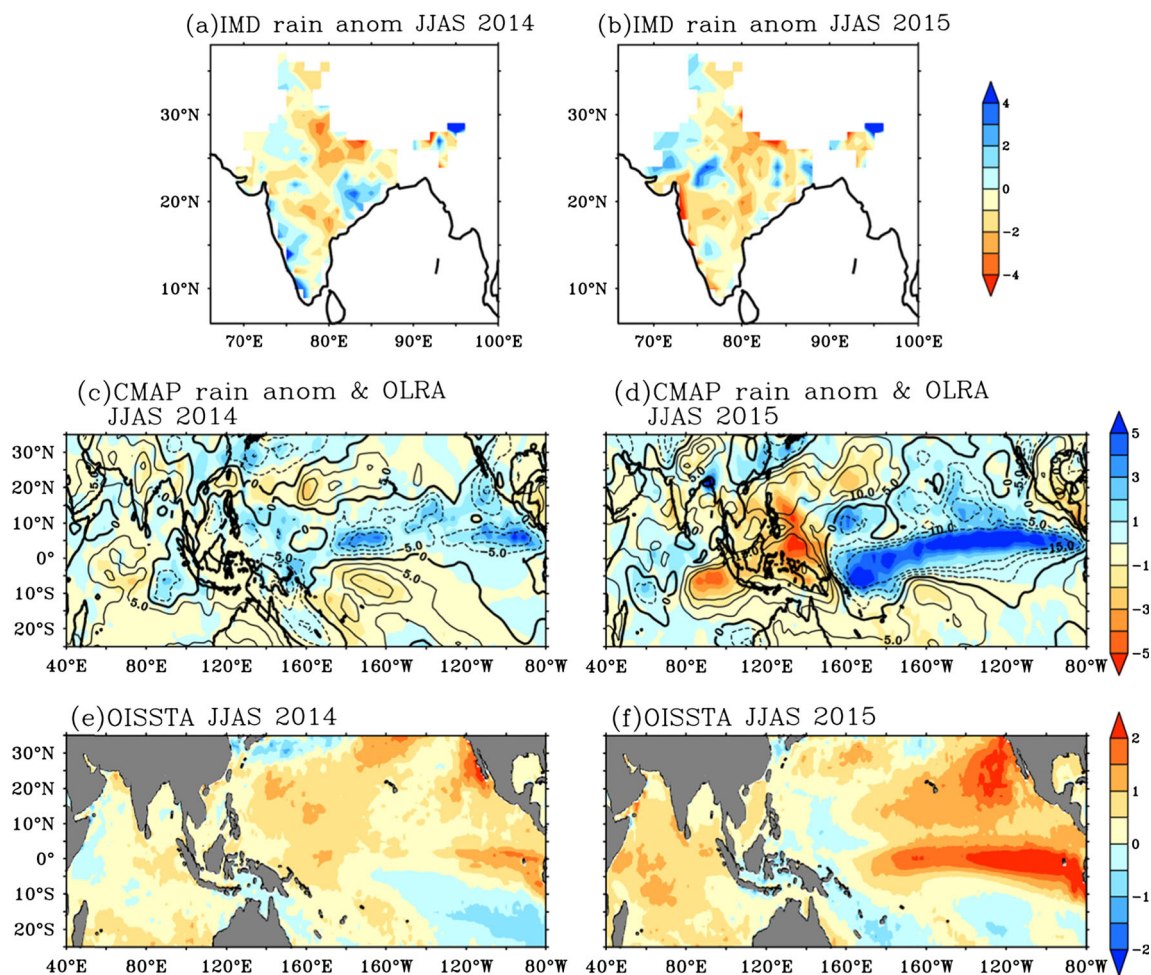

Fig. 1 **a** Precipitation anomalies (mm/day) based on IMD data. **c** Precipitation anomalies (mm/day) based on CMAP data (*shaded*) and OLR anomalies (W/m^2) (*contours*). **e** SST anomalies (°C) using OISST for JJAS 2014 (**b, d, f**) same as **a, c, e** but for JJAS 2015

Figure 2 shows the atmospheric features associated with the summer monsoon in both years. Positive SLP anomalies (Fig. 2a) are noted over the western TIO, whereas negative anomalies are seen over the region east of 80°E (up to east Pacific) and over the Indian land mass in 2014. A strong cross-equatorial flow reaching to the Western Ghats region and the associated positive rainfall (weak) anomalies are apparent in IMD and CMAP rainfall (Fig. 1a, c). Though SLP is low over the central north India, anomalous anticyclone between 20°N and 30°N and incursion of dry wind from north are primarily responsible for the deficient seasonal monsoon. Compared to 2014, pressure pattern and circulation are different in summer of 2015 over the ISM region though both years have received deficit rainfall. High-pressure anomalies over the Indian region and western Pacific and low pressure over the east Pacific are apparent in summer of 2015. Strong westerly wind anomalies in the equatorial Pacific are evident corresponding to the pressure differences. Rotational wind (Fig. 2b, e) showed low-level cyclonic circulation in the southeast Indian Ocean in 2014 but anticyclonic circulation in the same region in 2015. Associated with El Niño warming in central and eastern equatorial Pacific, upper-level divergence is seen in both years (Fig. 2c, f). As a result of strong El Niño, upper-level convergence or large-scale subsidence is located over the ISM region with maximum over the Maritime continent in 2015. In the case of the year 2014, associated with weak El Niño and warming over the western north Pacific, upper-level divergence is seen both over the western and eastern equatorial Pacific Ocean. Subsidence corresponding to this upper-level divergence is located over the western Indian Ocean in 2014. Over all, the summer of 2014 rainfall deficient is associated with anticyclonic circulation over central India, dry air incursion from north and the weak subsidence over some parts of India associated with Pacific warming. In the case of the year 2015, summer monsoon rainfall is suppressed mainly due to strong El Niño in the Pacific. This anomalous feature of the circulation enforces us to explore the status of dominant general circulation pattern of Walker and Hadley cells during these two years.

Changes in the warming patterns in the Indian Ocean and Pacific Ocean influence the ISM rainfall mainly through Walker and Hadley circulations. During El Niño, change in the heat source region in Pacific influences ISM rainfall through the thermally driven Walker Cell (Goswami et al.
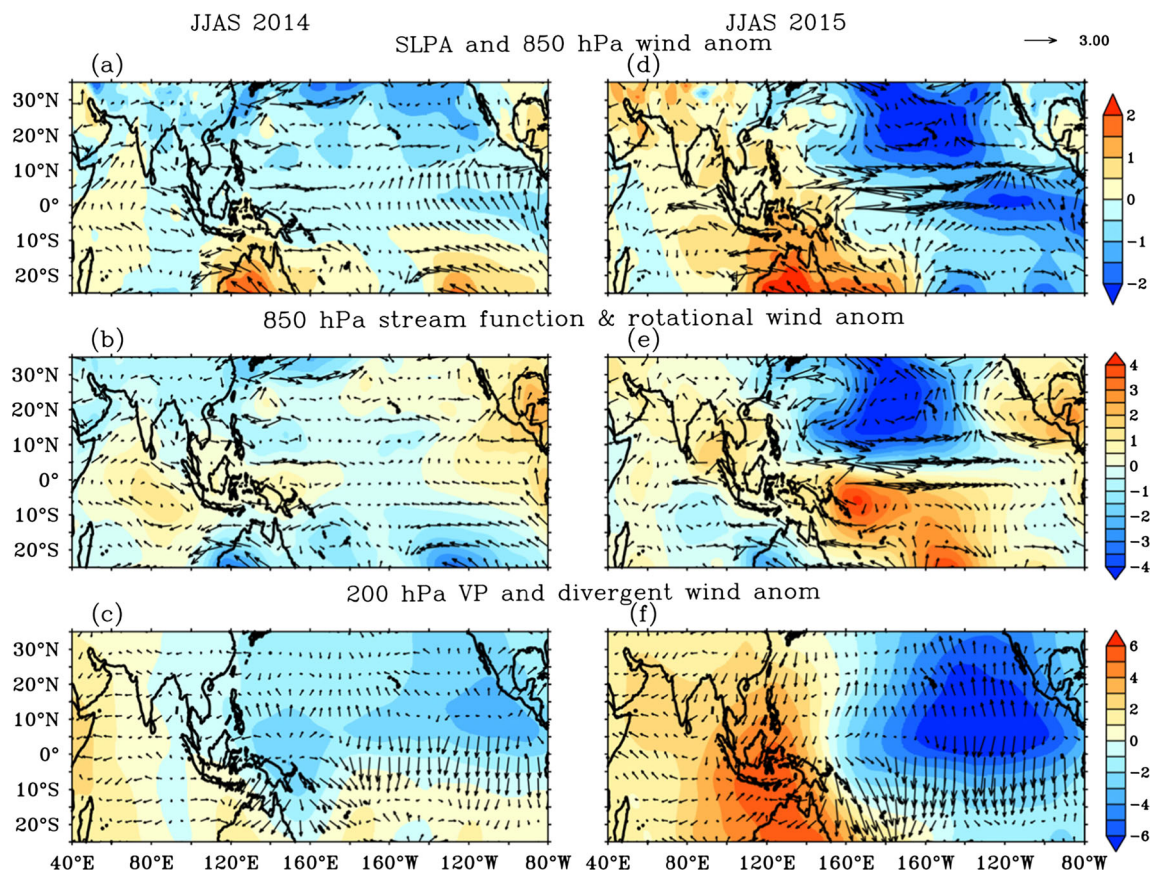

Fig. 2 a ERA Interim SLPA (hPa) (shaded) and ERA Interim 850 hPa wind (m/s) (vectors); b 850 hPa stream function (s^{-1}) (shaded) and rotational wind (m/s) (vector); c velocity potential (m^2/s) at 200 hPa (shaded) and divergent wind (m/s) at 200 hPa (vector) for JJAS 2014; and d, e, f are the same as a, b, c but for JJAS 2015

1999). Thus, understanding the changes in these two circulations is very important to study the mechanism responsible for the deficit ISM rainfall. Walker circulation anomalies averaged between 5°S to 5°N during 2014 and 2015 summer are illustrated in Fig. 3a, b, respectively. Strong upward motion in the central Pacific associated with anomalous warming and downward motion in the west Pacific and Indian Ocean is evident in summer 2015. This suggests that large-scale forcing from the Pacific has contributed largely to the deficient monsoon. However, during summer 2014, weak upward motion over the entire equatorial Pacific and eastern Indian Ocean (east of 95°E) and the subsidence or downward motion over the central and western Indian Ocean are noted.

The rainfall anomaly pattern clearly showed strong positive values just south of the equator over the eastern Indian Ocean in 2014 (Fig. 1c). Hadley circulation averaged between 95°E

and 100°E displays upward motion over the southeast equatorial Indian Ocean, and on the other hand, downward motion is seen from 5°N to 25°N (Fig. 3e). This indicates that low rainfall over the northeastern parts of India and Bangladesh in summer 2014 is influenced by local Hadley circulation. Positive rainfall anomalies and convection over the east equatorial Indian Ocean are supported by local SST warming (Fig. 1e). In the summer of 2015, strong downward motion is noted in the entire north Indian Ocean (Fig. 3f) unlike in 2014. This is mainly due to large-scale subsidence associated with El Niño.

Further, the longitude-height plot of zonal and vertical wind anomalies averaged over the North Indian Ocean (5°N to 25°N) region (Fig. 3c, d) showed strong upper-level westerly anomalies in 2015, suggesting weak easterly jet in the upper troposphere. Weak easterly jet over the ISM region in

Fig. 3 **a** Anomalous Walker Cell averaged over 5°S–5°N. **c** Anomalous Walker Cell averaged over 5°N –25°N. **e** Anomalous Hadley Cell averaged over 95°E–100°E using ERA-Interim data for JJAS 2014 and **b**, **d**, **f** are the same as **a**, **c**, **e** but for JJAS 2015
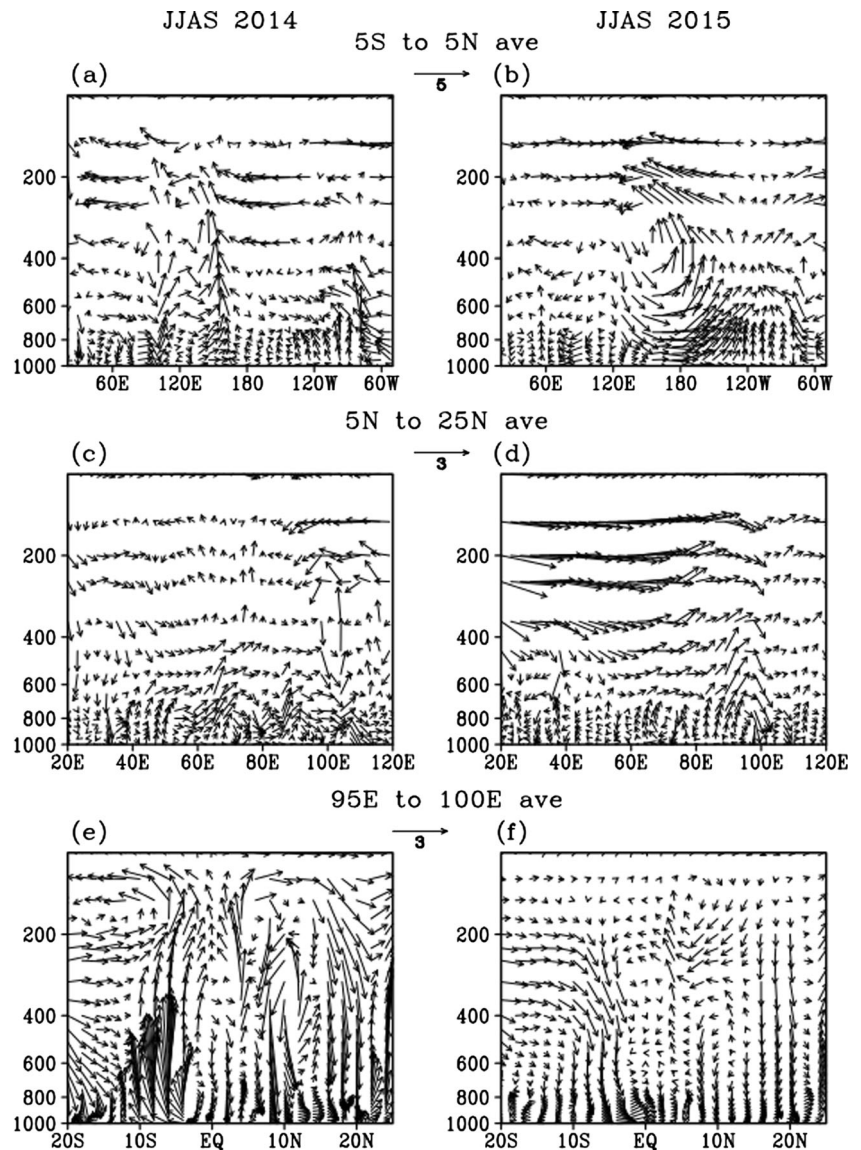
general is unfavourable for monsoon rainfall. In the case of year 2014, summer easterly jet is weak over the Arabian Sea region. In addition to that, the weak upward motion over the Indian land region centred on 80°E did not reach 500 mb to maintain deep convection. The circulation features in both 2014 and 2015 in general are not favourable for high rainfall over the ISM region. Thus, even though, 2014 and 2015 are ISM-deficit years, remote forcing from the Pacific and local circulation played different roles in the 2 years. Remote Pacific forcing due to El Niño resulted in less monsoon rainfall in 2015 through changes in the large-scale atmospheric circulation. Local circulation from northern latitudes, TIO SST and remote forcing from Pacific Ocean together influenced ISM rainfall in 2014.

It is well accepted that slowly, varying boundary conditions such as SST and upper ocean temperature are important for predicting ISM rainfall (e.g. Saha et al. 2016). The Pacific Ocean is warmer with strong (weak) El Niño in summer of 2015 (2014). Pacific SST warming has extended to the western basin in 2014 unlike in 2015. So, 2014 displayed a basin-wide warming feature whereas 2015 is more of a strong El Niño year. The eastern (western) equatorial Indian Ocean is anomalously warmer than the west (east) in summer 2014 (2015). These differences in SST in both Pacific and TIO seem to have considerable impact on ISM rainfall in 2014 and 2015 as discussed earlier. Thus, initializing forecast models with proper upper ocean temperature or SST distribution is essential. Further, how good the representation of the above-discussed SST patterns in the ocean assimilation system is important and needs to be addressed. These issues are studied in Sect. 4.

4 Representation of upper ocean temperature in IITM-GODAS

In this section, we examined how well the IITM-GODAS captures ocean temperature in the Indo-Pacific region during 2014 and 2015. Since GODAS is the ocean data assimilation system for CFSv2, we have compared ocean temperature features in IITM-GODAS with OISST and Had-EN4 product in the summer monsoon season. The evolution of surface and subsurface features from February to May is also examined to highlight its potential as a forecasting tool. It is important to note that representation of February to May are vital as seasonal prediction model ensembles are usually initialized in these months. The ability of IITM-GODAS in representing the observed oceanic features during JJAS makes it a potential tool to understand the ocean variability as well.

Figures 4a, b show SST anomalies over the Indo Pacific region respectively for JJAS 2014 and 2015. IITM-GODAS captured the JJAS-averaged SST anomalies very well in the 2 years as compared to OISST anomalies. The warm and cold

anomalies in IITM-GODAS were collocated with the OISST anomalies. Gradient in SST anomalies over the TIO region in 2014 is well represented in the model. The entire north Pacific (south of 30°N) displayed warming pattern in 2014 in both IITM-GODAS and OISST. In contrast, warm SST anomalies in the central and eastern Pacific and cold SST anomalies in the western Pacific are seen in 2015 and are consistent with the observations. It is also important to note strong warming of the entire northeast Pacific during 2015. Though TIO experienced basin-wide warming during 2014 and 2015, the amplitude of warming and the spatial distribution of anomalies are different. Significant anomalies are seen in the western TIO with strong warming only in 2015. It is known that over the El Niño region, surface and subsurface temperatures are well correlated (e.g. Harrison and Vecchi 2001; Zelle et al. 2004 Kug et al. 2010). Figure 4c, d show depth-longitude plots of temperature over the equatorial Pacific for both JJAS 2014 and 2015 in IITM-GODAS and Had-En4. The observed weak (strong) central and eastern subsurface warming in 2014 (2015) are well displayed in IITM-GODAS. Evolution of several indices of El Niño such as Niño 1 + 2, Niño 3, Niño 3.4 and Niño 4 along with IOD index during the years 2014 to 2015 are displayed in Fig. 5. Niño indices estimated using IITM-GODAS-based SST display correlation about 0.9 with the indices estimated from observed OISST. Though the plot is shown till September, skill score are based up to April 2016 which covers the whole cycle of El Niño 2015. This supports that IITM-GODAS could capture the evolution of Niño indices as in observation. This suggests that IITM-GODAS is able to provide better initial conditions to the coupled model CFSv2 for seasonal monsoon forecast.

The monthly evolution of anomalous SST from February to May in IITM-GODAS is displayed in Fig. 6. It is important to note that the anomalous SST patterns during the years 2014 and 2015 are well captured by IITM-GODAS. The anomalous surface warming over the central and east Pacific in 2015 in IITM-GODAS is consistent with the observations. From the first look, both 2014 and 2015 SST anomalies over the Pacific appear similar during February to May though there are differences in the TIO. But, the anomalous SST patterns underwent drastic changes especially over the Pacific during JJAS in both 2014 and 2015 with a basin-scale warming in 2014 and warming confined to east of 170°E in 2015 (Fig. 4). In order to reproduce the SST patterns in JJAS associated with El Niño, the model should capture the subsurface temperature evolution correctly in the previous season itself. Up and eastward propagation of subsurface temperature from February to summer season is very well represented in both the years though their magnitudes are weaker in 2014 compared to 2015 (Fig. 7). These initial conditionals are usually used to initialize seasonal forecasting system at IITM. It is important to note that IITM-GODAS compares well with Had-EN4 in 2015, whereas the eastern warming signals in the subsurface
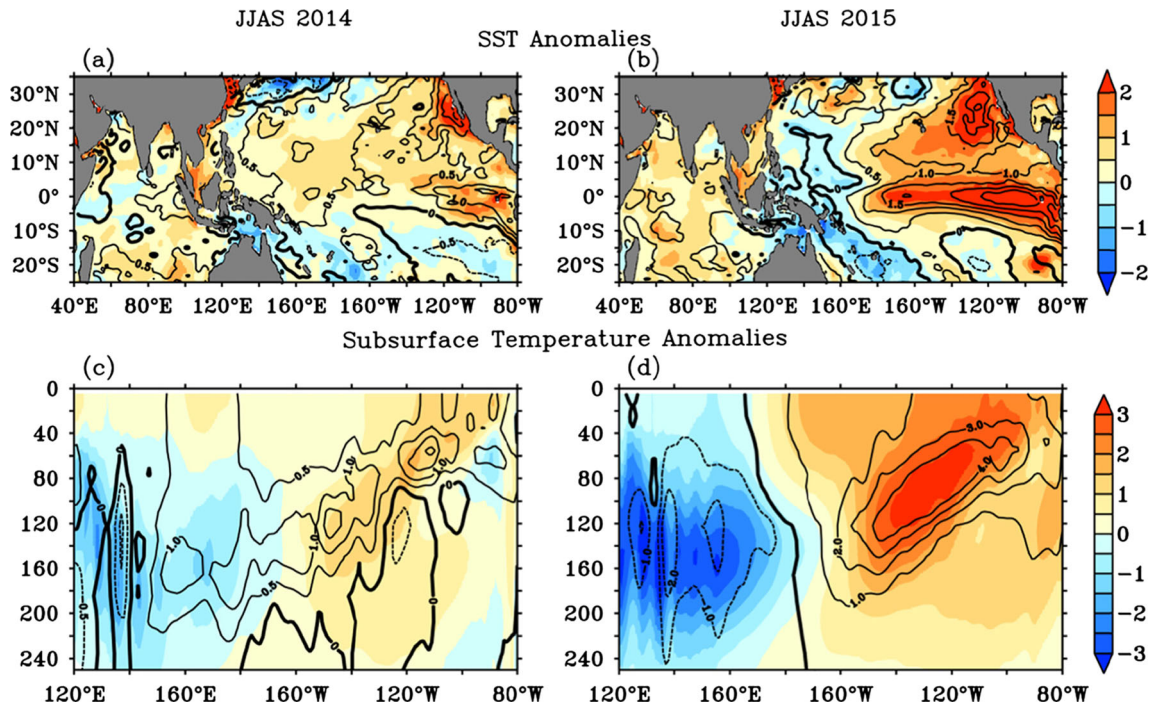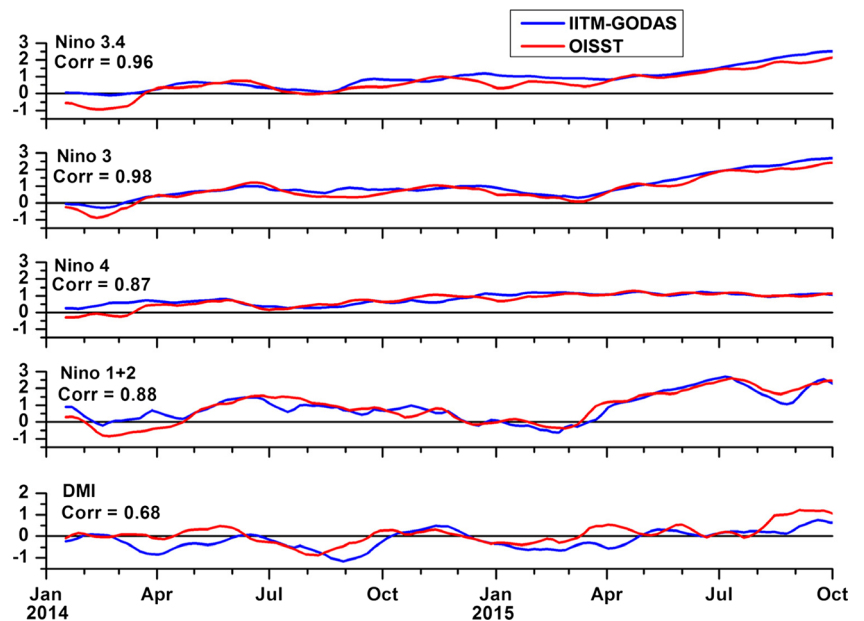
Fig. 4 **a** SST anomalies (°C) from IITM-GODAS (*shaded*) and OISST (*contours*) for JJAS 2014. **b** is the same as **a** but for JJAS 2015; **c**, **d** are the same as **a**, **b** but for subsurface temperature anomalies from IITM-GODAS (*shaded*) and Had-EN4 (*contours*) averaged over 5°S to 5°N

are weaker in IITM-GODAS than Had-EN4 in 2014. In addition to that, the subsurface cooling and its eastward extension in IITM-GODAS are much stronger than in Had-En4. So, the subsurface conditions in IITM-GODAS signal the weakening of El Niño much before the surface signals are observed.

Accurate surface wind forcing is very important for the ocean model to simulate correct SST and current patterns. IITM-GODAS is forced by NCMRWF winds. Westerly

wind bursts play an important role in the El Niño formation (e.g. Vecchi and Harrison, 2000). Thus, we have compared the time evolution of zonal wind anomalies from NCMRWF with ERA-Interim data in Fig. 8. The westerly wind burst in the western Pacific is evident from January to May 2014. In contrast to that, the easterly wind burst of June–July 2014 (Hu and Fedorov, 2016; Levine and McPhaden, 2016) is also captured well by NCMRWF

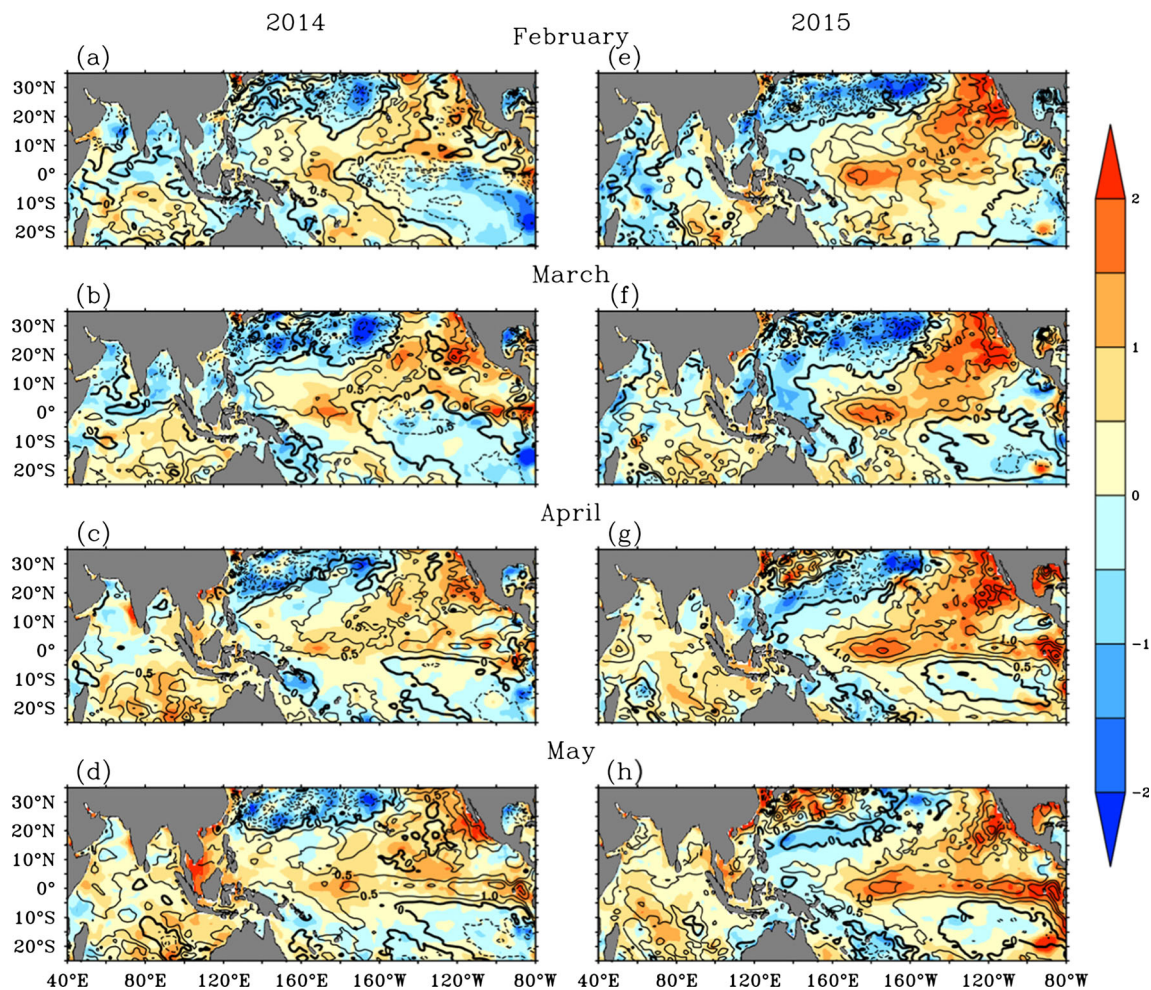**Fig. 5** 5-pentad running mean El Niño indices and DMI using IITM-GODAS and OISST

Fig. 6 SST anomalies (°C) from IITM-GODAS (*shaded*) and OISST (*contours*) from February to May (**a–d**) for 2014 and **e–h** for 2015

winds. The easterly wind anomalies in the eastern Pacific in NCMRWF forcing are in fact slightly stronger than that of ERA-Interim data. Westerly wind bursts in 2015 are also captured by NCMRWF winds. Figure 9 shows the time evolution of SST anomalies, upper ocean (average over 0 to 120 m) temperature anomalies and d20 anomalies using IITM-GODAS and other reanalysis products. The structure and strength of surface and subsurface features are well produced by IITM-GODAS. The eastward propagation of down-welling Kelvin waves associated with the westerly wind bursts is also seen in IITM-GODAS in 2015. The SST showed a zonal gradient with cold anomalies in the west and warm anomalies in the east causing more convergence in the Southeast Indian Ocean similar to Fig. 1. Basin-wide SST warming over the TIO in summer 2015 is also well represented by IITM-GODAS.

Overall, rainfall variations over the Indian subcontinent in 2014 and 2015 are mostly determined by the spatial distribution of tropical Pacific SST and partly from Indian Ocean. The IITM-GODAS which is assimilated with only ARGO temperature and salinity profiles could capture most of the observed

surface and subsurface temperature variations from early spring to summer in both 2014 and 2015.

As discussed above, IITM-GODAS is able to capture the ocean thermal structure during 2014 and 2015 over the Indo-Pacific region. It is important to examine the ISM seasonal rainfall patterns arising from these initial conditions in a coupled model, which is addressed here. CFSv2 hindcast experiments with IITM-GODAS ocean initial conditions (CFSv2-IITM-GODAS) are compared with CFSv2 experiment with NCEP initial conditions (CFSv2-NCEP-GODAS). Note that May initial conditions are used to generate JJAS rainfall patterns. Figure 10 shows the seasonal mean rainfall patterns over the ISM region for of 2014 and 2015. It can be seen that the IITM GODAS is showing the rainfall patterns at par of CFSv2-NCEP-GODAS). Also, improvement is seen over the Indian Ocean in CFSv2-IITM-GODAS). It is important to note that IITM GODAS assimilates only ARGO temperature and salinity profiles. Thus, only ARGO data assimilation gives the rainfall forecast similar to the one generated using the NCEP initial condition, in fact with some improvements over some regions. This highlights
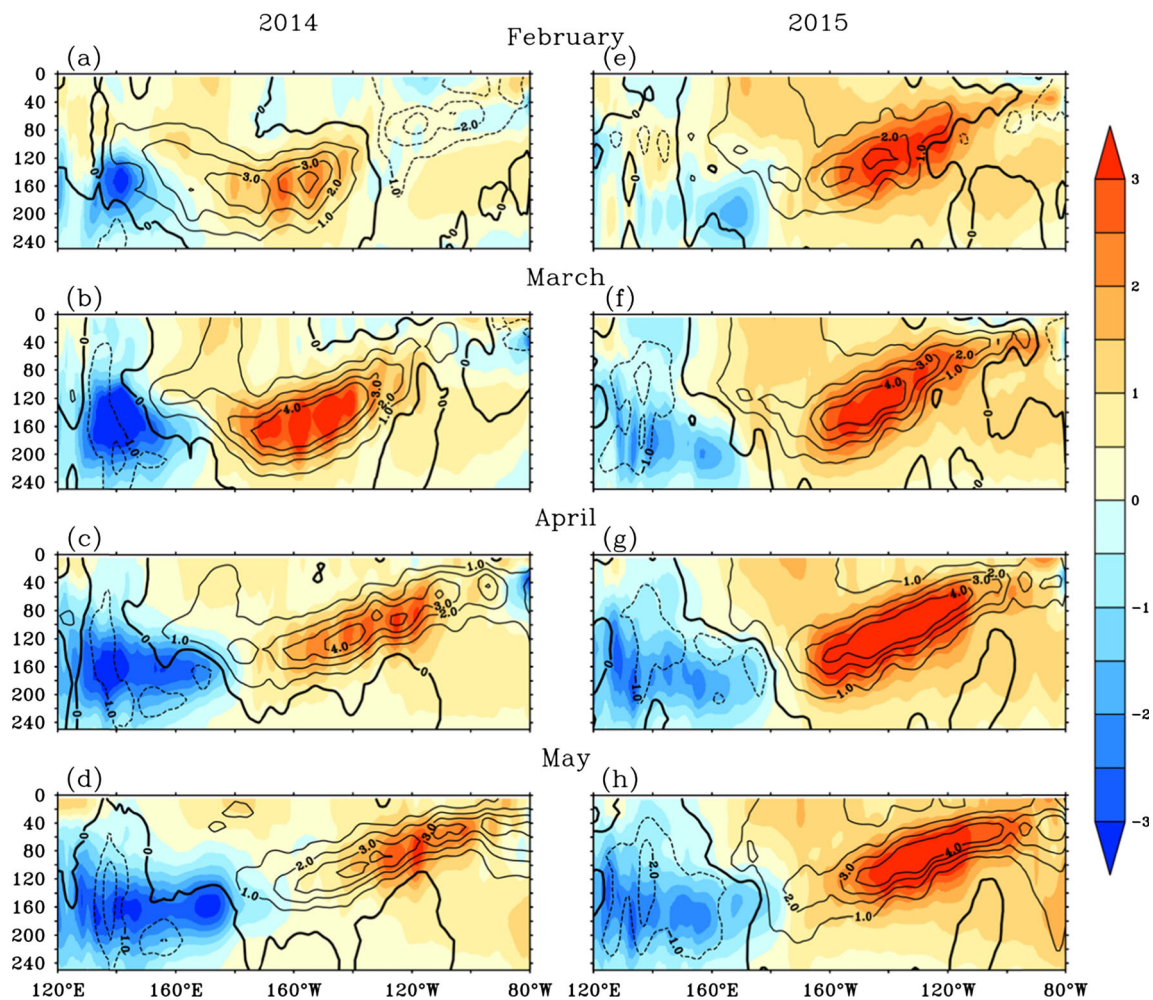
Fig. 7 Subsurface temperature anomalies (°C) averaged over 5°S to 5°N from IITM-GODAS (*shaded*) and Had-EN4 (*contours*) from February to May (**a–d**) for 2014 and **e–h** for 2015

the importance of the ARGO observation program on the regional climate modelling.

5 Summary

The present study addresses the factors responsible for the deficit ISM rainfall in 2014 and 2015. We have examined the remote SST forcing from the Pacific, local forcing from the Indian Ocean and associated atmospheric circulation changes and SLP patterns. We found significant differences in the local circulation in these two ISM rainfall-deficit years. Remote Pacific SSTs have impacted more in 2015 and both local circulation along with TIO SST and remote forcing from Pacific contributed in 2014.

In the summer of 2014, negative rainfall anomalies are evident over most of the Indian land region. The positive anomalies are seen over Western Ghats, Arabian Sea, southeast Indian Ocean and parts of Bay of Bengal off Orissa coast. The remaining parts of the Indian Ocean display negative

anomalies. Negative OLR anomalies collocated with positive rainfall anomalies in the southeast Indian Ocean reveal more convection over this region. On the other hand, weak negative SST anomalies are evident in the western equatorial Indian Ocean while the remaining parts of the Indian Ocean and most of the Pacific Ocean show warm anomalies. The western TIO shows positive SLP anomalies while most of the remaining region experiences negative anomalies. Anomalous anticyclone is evident over the central India in 2014, which plays a major role in the low rainfall in the central India. The upward branch of Hadley circulation averaged between 95°E and 100°E over the southeast equatorial Indian Ocean and downward branch over 5°N to 25°N suggest less precipitation over the northeastern parts of India.

The summer of 2015 also witnessed negative rainfall anomalies over most of the Indian land mass and also over the Arabian Sea and southeast Indian Ocean. On the other hand, negative OLR anomalies are evident in the southwest Indian Ocean. Strong El Niño-related warm SST anomalies over the central and eastern Pacific and cooling in the western

Fig. 8 Time evolution of zonal wind anomalies (m/s) averaged over 2°S to 2°N from **a** ERA Interim and **b** NCMRWF data

(a) ERA Interim u−wind anom

(b) NCMRWF u−wind anom
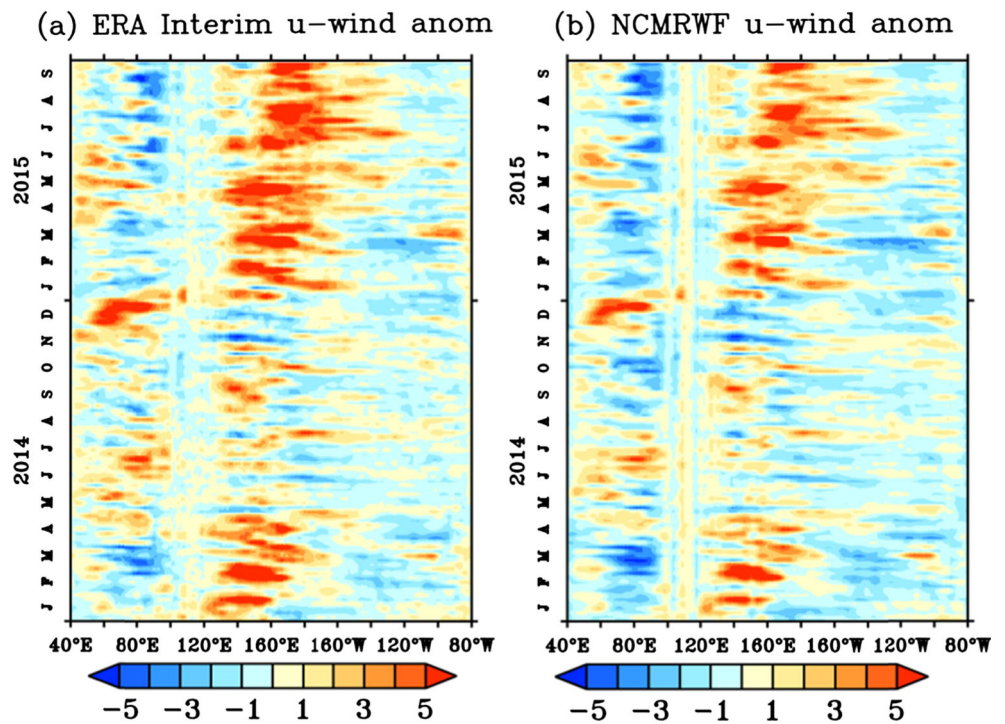
Pacific are evident in 2015. Indian Ocean experienced basin-wide warming in summer 2015, which is mainly induced by El Niño. Subsidence corresponding to El Niño induced changes in the Walker circulation is also located over this region with maximum over the Maritime continent in this year. Associated with this subsidence, strong downward motion is seen in the north Indian Ocean. These conditions have strong

impact on ISM rainfall. ISM rainfall is deficit over the Indian land in both 2014 and 2015. There are differences in the spatial distribution of rainfall over the Indian Ocean, SST anomalies and anomalous atmospheric circulations in the two years. A strong El Niño (remote Pacific Ocean) impacted ISM rainfall in 2015, but 2014 is modulated mainly by local circulation along with TIO and Pacific SST.
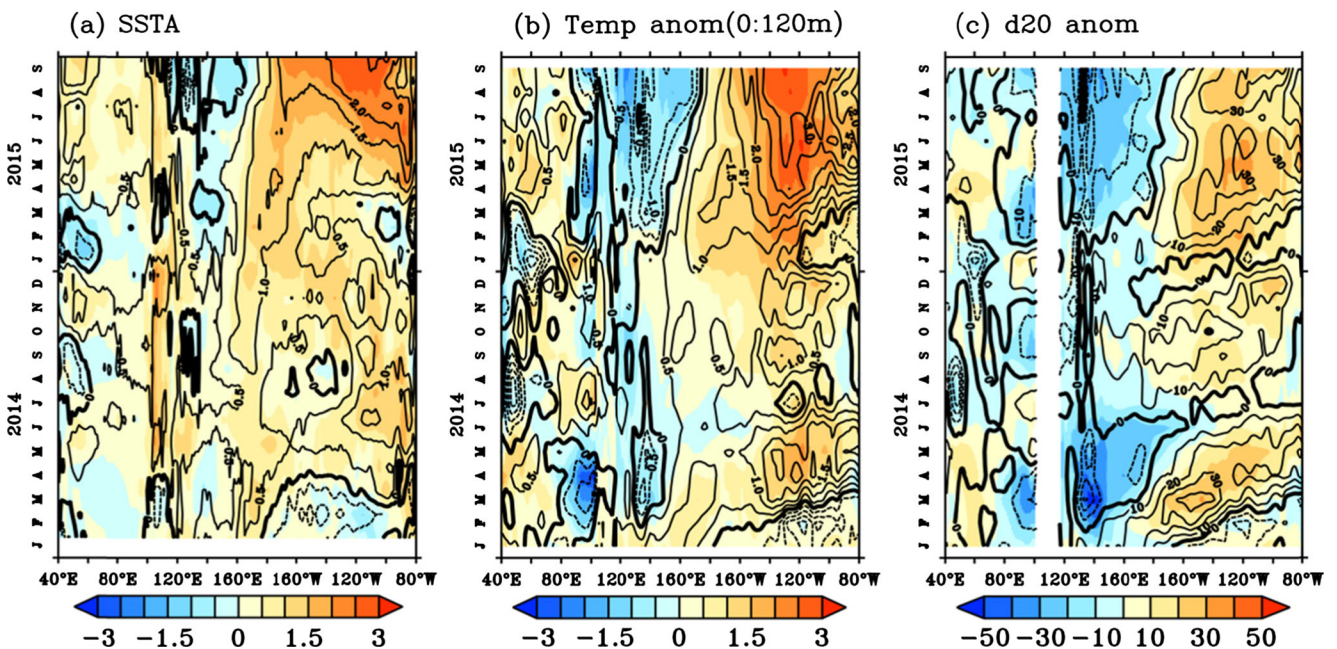

(a) SSTA

(b) Temp anom(0:120m)

(c) d20 anom

Fig. 9 Time evolution of **a** SST anomalies (°C) from IITM-GODAS (*shaded*) and OISST (*contours*) averaged over 5°S to 5°N. **b** Ocean temperature anomalies averaged over surface to 120 m and 5°S to 5°N

from IITM-GODAS (*shaded*) and Had-EN4 (*contours*). **c, d** 20 anomalies (m) from IITM-GODAS (*shaded*) and Had-EN4 (*contours*) averaged over 2°S to 2°N
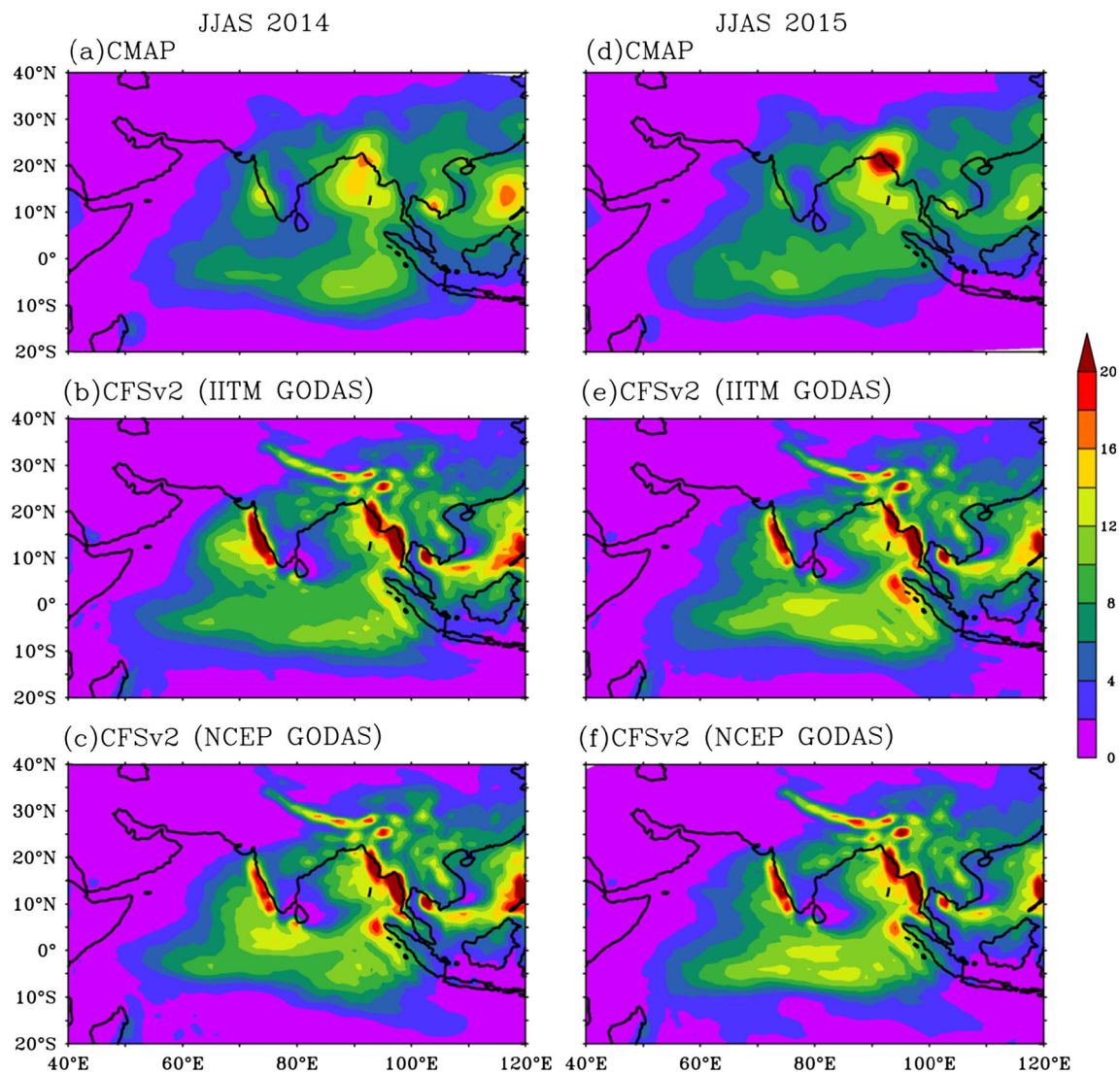
Fig. 10 JJAS mean rainfall over Indian summer monsoon region (mm/day) for 2014 (*left*) and 2015 (*right*). **a**, **d** CMAP; **b**, **e** CFSv2. Initialized with IITM GODAS and **c**, **f** CFSv2 initialized with NCEP GODAS

ISM is a coupled system in which ocean plays a critical role. Providing better ocean initial condition in a forecast model is vital for better forecast. We have examined the upper ocean thermal structure in IITM-GODAS which assimilates only ARGO temperature and salinity profiles. Since both Pacific and Indian Ocean SST impacted ISM rainfall in 2014 and 2015, it is essential to study how the IITM-GODAS captures the upper ocean thermal structure in the Indo-Pacific region. IITM-GODAS well captured the seasonal and also monthly SST and subsurface temperature compared to reanalysis products and observations. Evolution of all the four Niño indices and DMI are comparable with the observations. The eastward propagation of downwelling Kelvin wave which is important for El Niño development is also seen in IITM-GODAS in 2015 similar to that of Had-EN4. IITM-GODAS

with only ARGO data assimilation could capture the ocean state responsible for the deficit ISM rainfall in 2014 and 2015, highlighting the importance of ARGO observational network for monsoon forecast.

References

Ananthakrishnan R (1970) Reversal of pressure gradients and wind circulation across India and the southwest monsoon. Quart J R Met Soc 96:539–542

Ashok K, Guan Z, Yamagata T (2001) Impact of the Indian Ocean dipole on the relationship between the Indian monsoon rainfall and ENSO. Geophys Res Lett 28(23):4499–4502

Balmaseda M, Anderson D (2009) Impact of initialization strategies and observations on seasonal forecast skill. Geophys Res Lett 36: L01701. doi:10.1029/2008GL035561

Balmaseda M, Anderson D, Vidard A (2007) Impact of ARGO on analyses of the global ocean. Geophys Res Lett 34:L16605. doi:10.1029/2007GL030452

Balmaseda MA, Alves OJ, Arribas A, Awaji T, Behringer DW, Ferry N, Fujii Y, Lee T, Rienecker M, Rosati T, Stammer D (2009) Ocean initialization for seasonal forecasts. Oceanography 22(3):154–159. doi:10.5670/oceanog.2009.73

Bawiskar SM (2009) Weakening of lower tropospheric temperature gradient between Indian landmass and neighbouring oceans and its impact on Indian monsoon. J Earth Syst Sci 118(4):273–280

Behringer DW (2007) The Global Ocean Data Assimilation System at NCEP, paper presented at the 11th Symposium on Integrated Observing and Assimilation Systems for Atmosphere, Oceans, and Land Surface, Am. Meteorol. Soc., San Antonio, Tex

Behringer DW, Xue Y (2004) Evaluation of the global ocean data assimilation system at NCEP: the Pacific Ocean. Eighth symposium on integrated observing and assimilation system for atmosphere, ocean, and land surface, AMS 84th annual meeting, 11–15

Chowdary JS, Bandgar AB, Gnanaseelan C, Luo J-J (2015) Role of tropical Indian Ocean air–sea interactions in modulating Indian summer monsoon in a coupled model. Atmos Sci Let 16:170–176. doi:10.1002/asl2.561

Dee DP, Uppala SM, Simmons AJ, Berrisford P, Poli P, Kobayashi S, Andrae U, Balmaseda MA, Balsamo G, Bauer P, Bechtold P, Beljaars ACM, van de Berg L, Bidlot J, Bormann N, Delsol C, Dragani R, Fuentes M, Geer AJ, Haimberger L, Healy SB, Hersbach H, Holm EV, Isaksen L, Kallberg P, Kohler M, Matricardi M, McNally AP, Monge-Sanz BM, Morcrette J-J, Park B-K, Peubey C, de Rosnay P, Tavolato C, Thepaut J-N, Vitart F (2011) The ERA-interim reanalysis: configuration and performance of the data assimilation system. Q J R Meteorol Soc 137:553–597

Gadgil S, Vinayachandran PN, Francis PA, Gadgil S (2004) Extremes of the Indian summer monsoon rainfall, ENSO and equatorial Indian Ocean oscillation. Geophys Res Lett 31:L12213. doi:10.1029/2004GL019733

Gadgil S, Rajeevan M, Francis PA (2007) Monsoon variability: links to major oscillations over the equatorial Pacific and Indian oceans. Current Science Special Section: Indian Monsoon 93(2):182–194

Good SA, Martin MJ, Rayner NA (2013) EN4: quality controlled ocean temperature and salinity profiles and monthly objective analyses with uncertainty estimates. J Geophys Res: Oceans 118:6704–6716. doi:10.1002/2013JC009067

Goswami BN, Krishnamurthy V, Annamalai H (1999) A broadscale circulation index for interannual variability of the Indian summer monsoon. Q J R Meteorol Soc 125:611–633

Gould J, Roemmich D, Wijffels S, Freeland H, Ignaszewsky M, Jianping X, Pouliquen S, Desaubies Y, Send U, Radhakrishnan K, Takeuchi K, Kim K, Danchenkov M, Sutton P, King B, Owens B, Riser S (2004) ARGO profiling floats bring new era of in Situ Ocean observations. Eos 85(19):185–191. doi:10.1029/2004EO190002

Griffies SM, Harrison MJ, Pacanowski RC, Rosati A (2004) A technical guide to MOM4. NOAA/Geophysical Fluid Dynamics Laboratory, Princeton, USA, 337 pp

Harrison DE, Vecchi GA (2001) El Niño and La Niña—equatorial Pacific thermocline depth and sea surface temperature anomalies, 1986-98. Geophys Res Lett 28(6):1051–1054

Hu S, Fedorov AV (2016) Exceptionally strong easterly wind burst stalling el Niño of 2014. Proc Natl Acad Sci U S A 113(8):2005–2010

Ji M, Leetmaa A (1997) Impact of data assimilation on ocean initialization and El Niño prediction. Mon Weath Rev 125:742:753

Ji M, Behringer W, Leetmaa A (1998) An improved coupled model for ENSO prediction and implications for ocean initialization. Part II: the coupled model. Mon Weath Rev 126:1022–1034

Jiang X, Yang S, Li Y, Kumar A, Liu X, Zuo Z, Zha B (2013) Seasonal-to-interannual prediction of the Asian summer monsoon in the NCEP climate forecast system version 2. J Clim 26:3708–3727. doi:10.1175/JCLI-D-12-00437.1

Keshavamurthy RN (1982) Response of the atmosphere to sea surface temperature anomalies over the equatorial Pacific and the teleconnections of the southern oscillation. J Atmos Sci 39:1241–1259

Khandekar R, Gnanaseelan C, Swapna P, Parekh A, Sreenivas P, Srinivas G, Chowdary JS, Deepa JS (2015) Oceanic features in the Indo-Pacific region during the southwest monsoon 2015. In: Mujumdar M, Gnanaseelan C, Rajeevan M (eds) A Research Report on the 2015 Southwest Monsoon. IITM Scientific (Research) Report, pp14–22, ISSN 0252–1075, ESSO/IITM/ SERP/SR/02(2015)/185

Kim H-M, Webster PJ, Curry JA, Toma VE (2012) Asian summer monsoon prediction in ECMWF system 4 and NCEP CFSv2 retrospective seasonal forecasts. Clim Dyn 39:2975–2991. doi:10.1007/s00382-012-1470-5

Kothawale DR, Kulkarni JR (2014) Performance of all-India southwest monsoon seasonal rainfall when monthly rainfall reported as deficit/ excess. Meteorol Appl 21:619–634. doi:10.1002/met.1385

Kothawale DR, Munot AA, Borgaonkar HP (2008) Temperature variability over the Indian Ocean and its relationship with Indian summer monsoon rainfall. Theor. Appl Climatol 92:31–35. doi:10.1007/s00704-006-0291-z

Kripalani RH, Kulkarni A (1997) Climatic impact of El-Niño/La Niña on the Indian monsoon: a new perspective. Weather 52:39–46

Krishnan R, Ramesh KV, Samala BK, Meyers G, Slingo JM, Fennessy MJ (2006) Indian Ocean-monsoon coupled interactions and impending monsoon droughts. Geophys Res Lett 33:L08711. doi:10.1029/2006GL025811

Kug J-S, Choi J, An S-I, Jin F-F, Wittenberg AT (2010) Warm pool and cold tongue El Niño events as simulated by the GFDL 2.1 coupled GCM. J Clim 23:1226–1239. doi:10.1175/2009JCLI3293.1

Kumar KK, Rajagopalan KB, Cane MA (1999) On the weakening relationship between the Indian monsoon and ENSO. Science 284:2156–2159

Kumar KK, Rajagopalan B, Hoerling M, Bates G, Cane M (2006) Unraveling the mystery of Indian monsoon failure during El Niño. Science 314:115–119. doi:10.1126/science.1131152

Lee H-T and NOAA CDR Program (2011): NOAA climate data record (CDR) of monthly outgoing longwave radiation (OLR), Version 2.2–1. NOAA National Climatic Data Center. doi:10.7289/V5222RQP

Levine AFZ, McPhaden MJ (2016) How the July 2014 easterly wind burst gave the 2015-2016 El Niño a head start. Geophys Res Lett 43:6503–6510. doi:10.1002/2016GL069204

Levitus S, Antonov JI, Boyer TP, Locarnini RA, Garcia HE, Mishonov AV (2009) Global ocean heat content 1955-2008 in light of recently revealed instrumentation problems. Geophy Res Lett 36:L07608. doi:10.1029/2008GL037155

Pai DS, Bhan SC (2015) Monsoon 2014: a report. IMD Met. Monograph: ESSO Document No.: ESSO/IMD/Synoptic Met./01(2015)/17

Pai DS, Sridhar L, Rajeevan M, Sreejith OP, Satbhai NS, Mukhopadhyay B (2014) Development of a new high spatial resolution

(0.25° × 0.25°) long period (1901-2010) daily gridded rainfall data set over India and its comparison with existing data sets over the region. Mausam 65(1):1–18

Pant GB, Parthasarathy B (1981) Some aspects of an association between the southern oscillation and Indian summer monsoon. A Met Geophy Biokl Ser B 29:245–251

Rasmusson EM, Carpenter TH (1983) The relationship between eastern equatorial Pacific Sea surface temperature and rainfall over India and Sri Lanka. Mon Weather Rev 111:517–528

Ravichandran M, Behringer D, Sivareddy S, Girishkumar MS, Neethu C, Harikumar R (2011) INCOIS-GODAS-MOM: ocean analysis for the Indian Ocean: configuration, validation and product dissemination. Technical Report Report No.: INCOIS-MOG-TR-2011-06

Ravichandran M, Behringer D, Sivareddy S, Girishkumar MS, Chacko N, Harikumar R (2013) Evaluation of the Global Ocean data assimilation system at INCOIS: the tropical Indian Ocean. Ocean Model 69:123–135

Reynolds RW, Smith TM, Liu C, Chelton DB, Casey KS, Schlax MG (2007) Daily high-resolution-blended analyses for sea surface temperature. J Clim 20:5473–5496. doi:10.1175/2007JCLI1824.1

Roemmich D, Gilson J (2009) The 2004–2008 mean and annual cycle of temperature, salinity, and steric height in the global ocean from the ARGO program. Prog Oceanogr 82:81–100. doi:10.1016/j.pocean.2009.03.004

Roemmich D, Gilson J (2011) The global ocean imprint of ENSO. Geophys Res Lett 38:L13606. doi:10.1029/2011GL047992

Roemmich D et al. (the Argo Science Team) (1998) On the design and implementation of ARGO: an initial plan for a global array of profiling floats. International CLIVAR Project Office Report 21, GODAE International Project Office, Melbourne, Australia, 32 pp

Ropelewski CP, Halpert MS (1987) Global and regional scale precipitation patterns associated with the El Niño/southern oscillation. Mon Weather Rev 115:1606–1626

Saha S, Moorthi S, Wu X, Wang J, Nadiga S, Tripp P, Behringer D, Hou Y-T, Chuang H, Iredell M, Ek M, Meng J, Yang R, MendezMP, Dool HVD, ZhangQ, WangW, ChenM, Becker E (2014) The NCEP climate forecast system version 2. J Clim 27: 2185–2208

Saha SK, Pokhrel S, Salunke K, Dhakate A, Chaudhari HS, Rahaman H, Sujith K, Hazra A, Sikka DR (2016) Potential predictability of Indian summer monsoon rainfall in NCEP CFSv2. J Adv Model Earth Syst 8:96–120. doi:10.1002/2015MS000542

Saji NH, Goswami BN, Vinayachandran PN, Yamagata T (1999) A dipole mode in the tropical Indian Ocean. Nature 401:360–363

Shukla J (1975) Effect of Arabian Sea-surface temperature anomaly on Indian summer monsoon: a numerical experiment with the GFDL model. J Atmos Sci 32:503–511

Sreenivas P, Gnanaseelan C, Kakatkar R, Pavan Kumar N, Chowdary JS, Parekh A, Singh P (2015) Implementation and validation of Global Ocean Data Assimilation System at IITM. IITM Scientific (Research) Report, ISSN 0252–1075, ESSO/IITM/SERP/SR/01(2015)/184

Trenberth KE, Hurrell JW, Stepaniak DP (2006) The Asian Monsoon: global perspectives. In: Wang B (ed) The Asian Monsoon. Springer, Praxis Publishing Ltd., UK, pp 67–87

Varikoden H, Singh BB, Sooraj KP, Joshi MK, Preethi B, Mujumdar M, Rajeevan M., (2015), Large scale features of southwest monsoon during 2015. In: Mujumdar M, Gnanaseelan C, Rajeevan M (ed) A Research Report on the 2015 Southwest Monsoon. IITM Scientific (Research) Report, pp 2–13, ISSN 0252–1075, ESSO/IITM/SERP/SR/02(2015)/185

Vecchi GA, Harrison DE (2000) Tropical Pacific Sea surface temperature anomalies, El Niño, and equatorial westerly wind events. J Clim 13: 1814–1830

Webster PJ (2006) The coupled monsoon system. In: Wang B (ed) The Asian Monsoon. Springer, Praxis Publishing Ltd., UK, pp 3–66

Webster PJ, Chou LC (1980) Seasonal structure of a simple monsoon system. J Atms Sci 37:354–367

Webster PJ, Magana VO, Palmer TN, Shukla J, Tomas RA, Yanai M, Yasunari T (1998) Monsoons: processes, predictability, and the prospects for prediction. J Geophys Res 103(C7):14451–14510

Xie P, Arkin PA (1997) Global precipitation: a 17-year monthly analysis based on gauge observations, satellite estimates, and numerical model outputs. Bull Amer Meteor Soc 78:2539–2558

Yang S, Zhang Z, Kousky VE, Higgins RW, Yoo S-H, Liang J, Fan Y (2008) Simulations and seasonal prediction of the Asian summer monsoon in the NCEP climate forecast system. J Clim 21:3755–3775. doi:10.1175/2008JCLI1961.1

Zelle H, Appeldoorn G, Burgers G, Oldenborgh GJV (2004) The relationship between sea surface temperature and thermocline depth in the eastern equatorial Pacific. J Phys Oceanogr 34:643–655